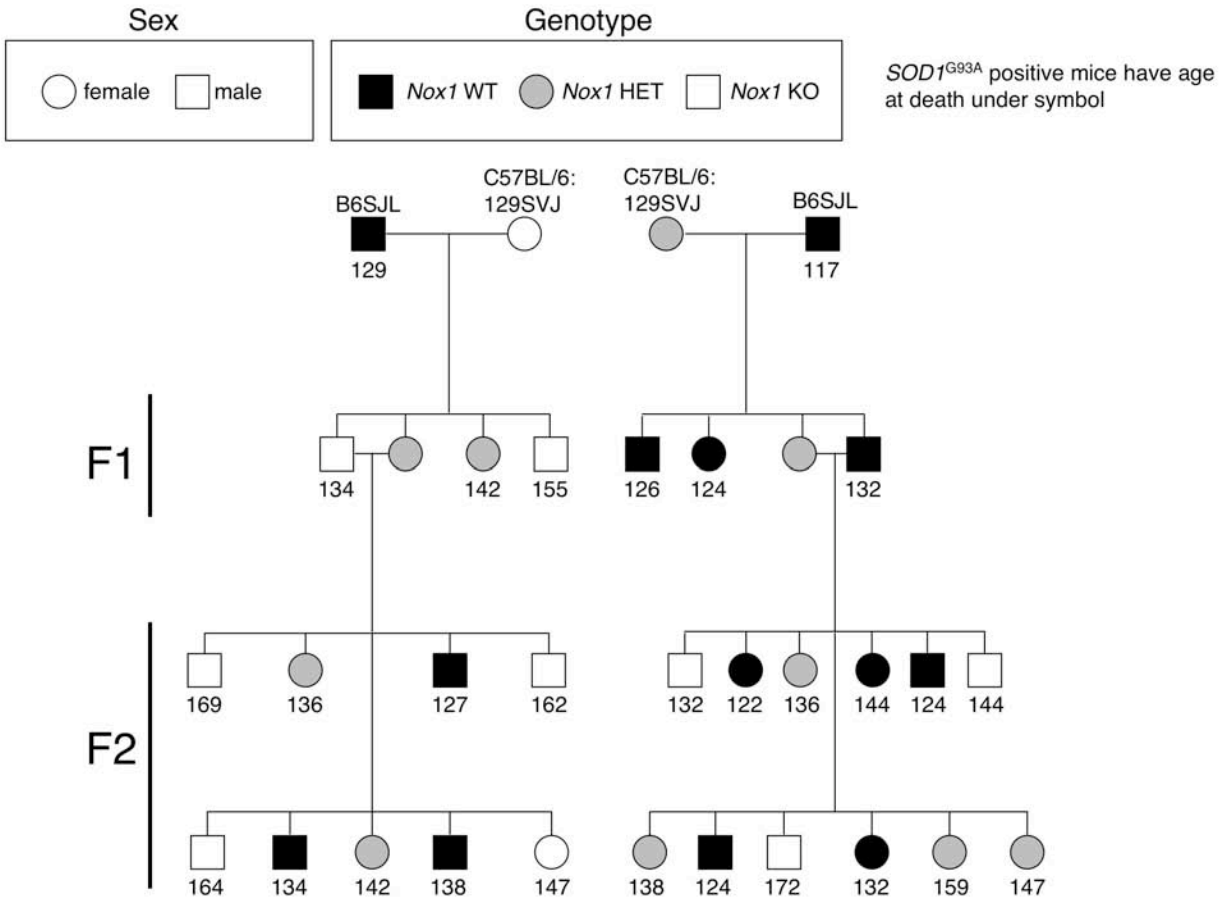

Figure S1. Schematic depicting the lineage of the *SOD1*^{G93A} transgenic mice on the *Nox1* knockout background. Age at which *SOD1*^{G93A} transgenic mice reached clinical death is listed under the symbol. Data from both F1 and F2 generations is given and with the exception of the founders, only *SOD1*^{G93A} transgenic mice derived from breedings are shown.

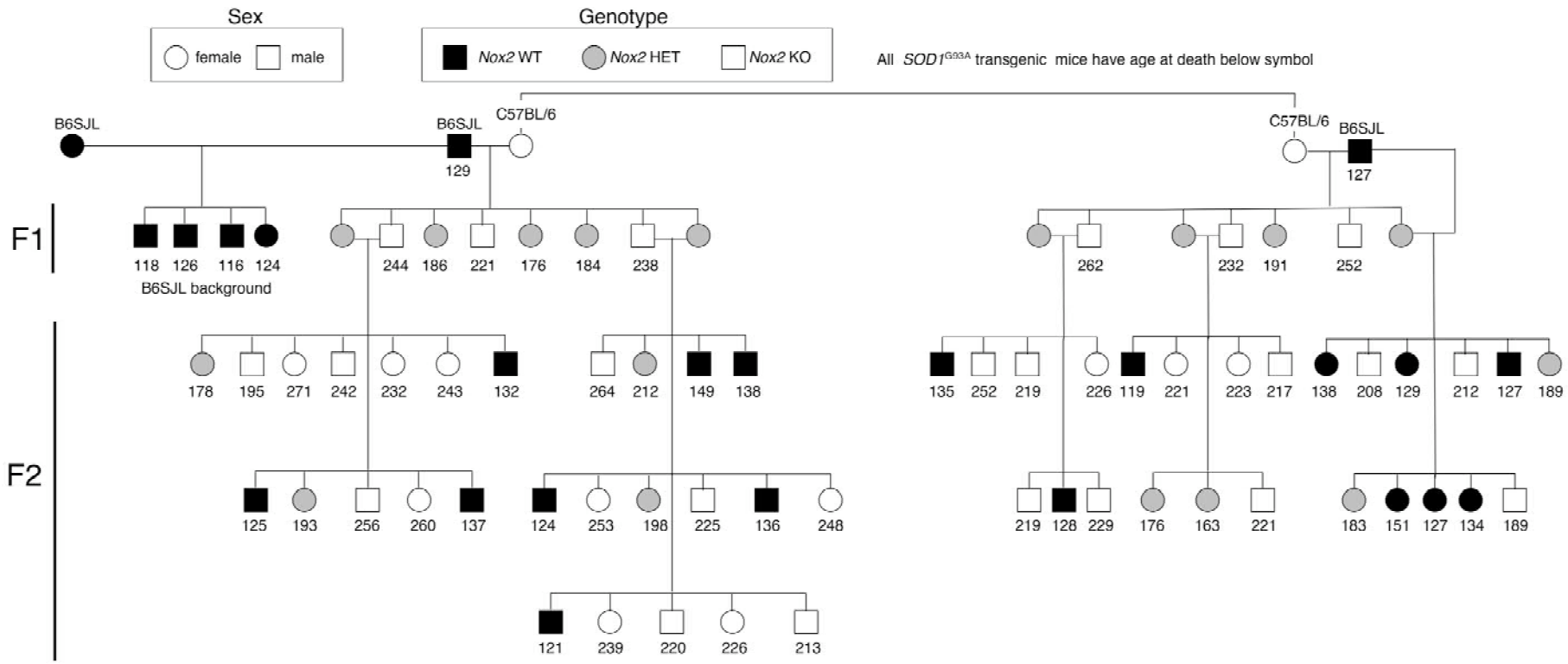

Figure S2. Schematic depicting the lineage of the *SOD1*^{G93A} transgenic mice on the *Nox2* knockout background. Age at which *SOD1*^{G93A} transgenic mice reached clinical death is listed under the symbol. Data from both F1 and F2 generations is given and with the exception of the founders, only *SOD1*^{G93A} transgenic mice derived from breedings are shown.

A

Genotype	*mIL2* CT	*hSOD1* CT	△ CT	Transgene Copies
SOD1^{G93A}-*Nox2* WT	25.46	18.63	6.83	22.04 +/- 0.7
SOD1^{G93A}-*Nox2* Het	27.12	20.16	6.95	21.57 +/- 0.98
SOD1^{G93A}-*Nox2* KO	25.92	19.07	6.85	22.26 +/- 0.60

B

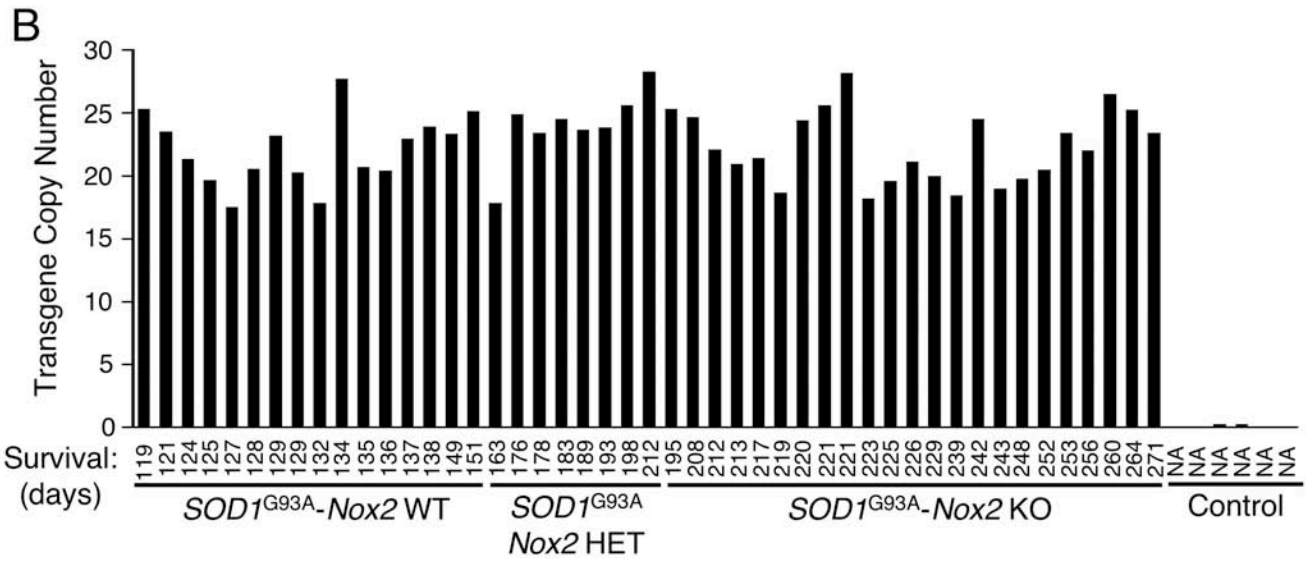

Figure S3. Mutant *SOD1*^{G93A} transgene copy number for each mouse in the F2 generation of the *Nox2* cohort was determined using quantitative real-time PCR. (**A**) Averages for CT, ΔCT, and transgene copies are given for each genotype of mice. (**B**) Graph depicting copy number versus age of survival for each mouse in the cohort. Control mice were *hSOD1* transgene negative and were not monitored for survival. One *SOD1*^{G93A} *Nox2*-knockout mouse (which survived to 185 days) is omitted because tail DNA was of an insufficient quality to generate valid *IL2* CT values and we did not have other tissue to repeat the studies.

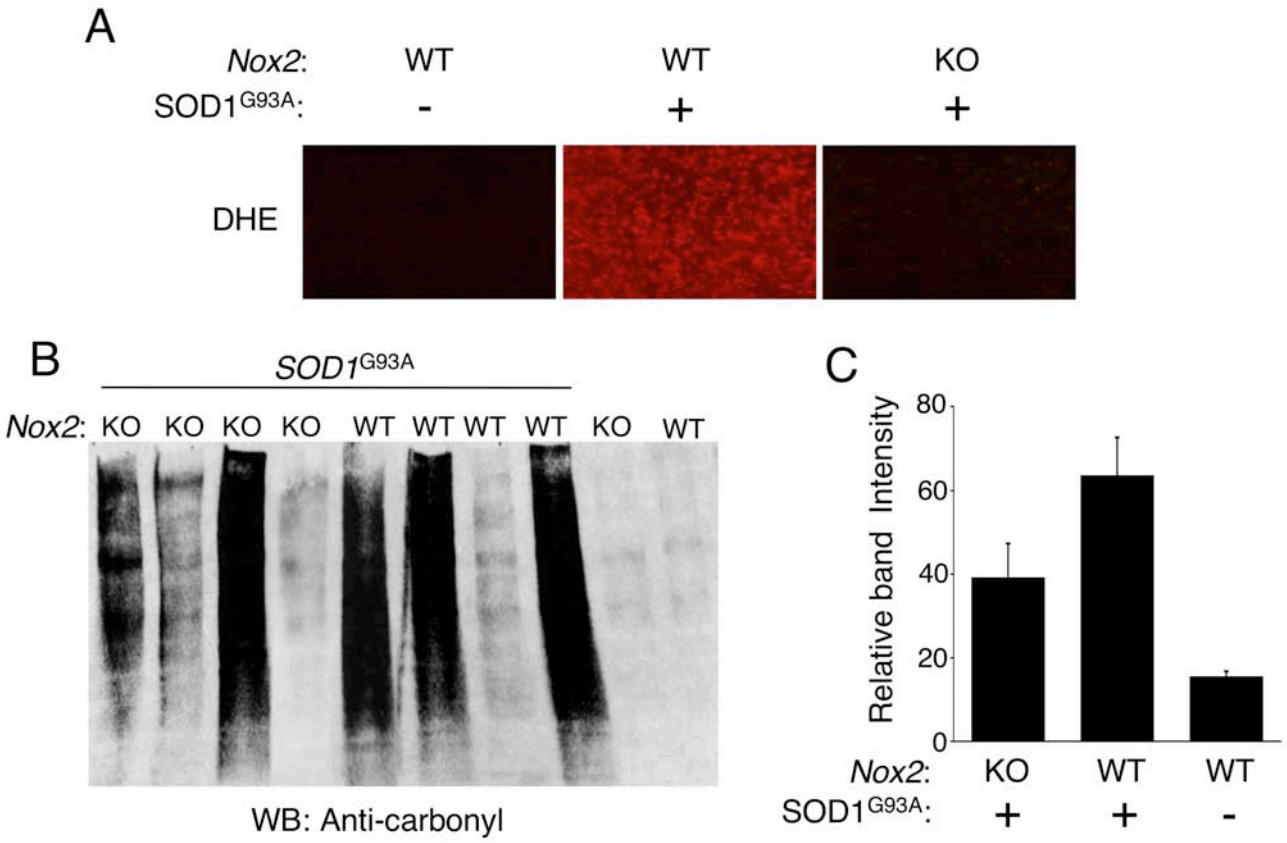

Figure S4. Redox stress in the spinal cord of *SOD1*^{G93A} *Nox2*-knockout mice. **(A)** Dihydroethidium fluorescence in 30 μm sections of spinal cord from 120 day-old age-matched *SOD1*^{G93A}/*Nox2*-WT, *SOD1*^{G93A}/*Nox2*-KO, and non-transgenic mice. Magnification bar is equal to 100 μm. **(B)** Western blotting for protein carbonyl adducts in spinal cord homogenates treated with 2,4 dinitrophenylhydrazine from 120 day-old age-matched *SOD1*^{G93A}/*Nox2*-WT, *SOD1*^{G93A}/*Nox2*-KO, and non-transgenic mice. Four mice were assessed per genotype. **(C)** Quantification of band intensity from (B) using Image J software. Although there was not a significant difference between the *SOD1*^{G93A}/*Nox2*-KO and *SOD1*^{G93A}/*Nox2*-WT, there was a trend of reduced carbonylation in the *SOD1*^{G93A}/*Nox2*-KO samples. *Methods for DHE staining:* Mice were euthanized with an overdose of sodium pentobarbital. The lumbar spinal cord was removed immediately and embedded in OTC as 4 mm-long segments. 30 mm section from each group were immediately generated within hours of embedding and stained in 1 μM dihydroethidium (DHE) in PBS for 5 minutes in the dark. Sections were then rinsed in PBS and coverslipped with Vectashield mounting media containing DAPI. DHE fluorescence was detected using a rhodamine emission filter. Microscope/camera exposure settings were kept constant between samples within an individual experiment, and control and experimental animals were always processed in parallel.

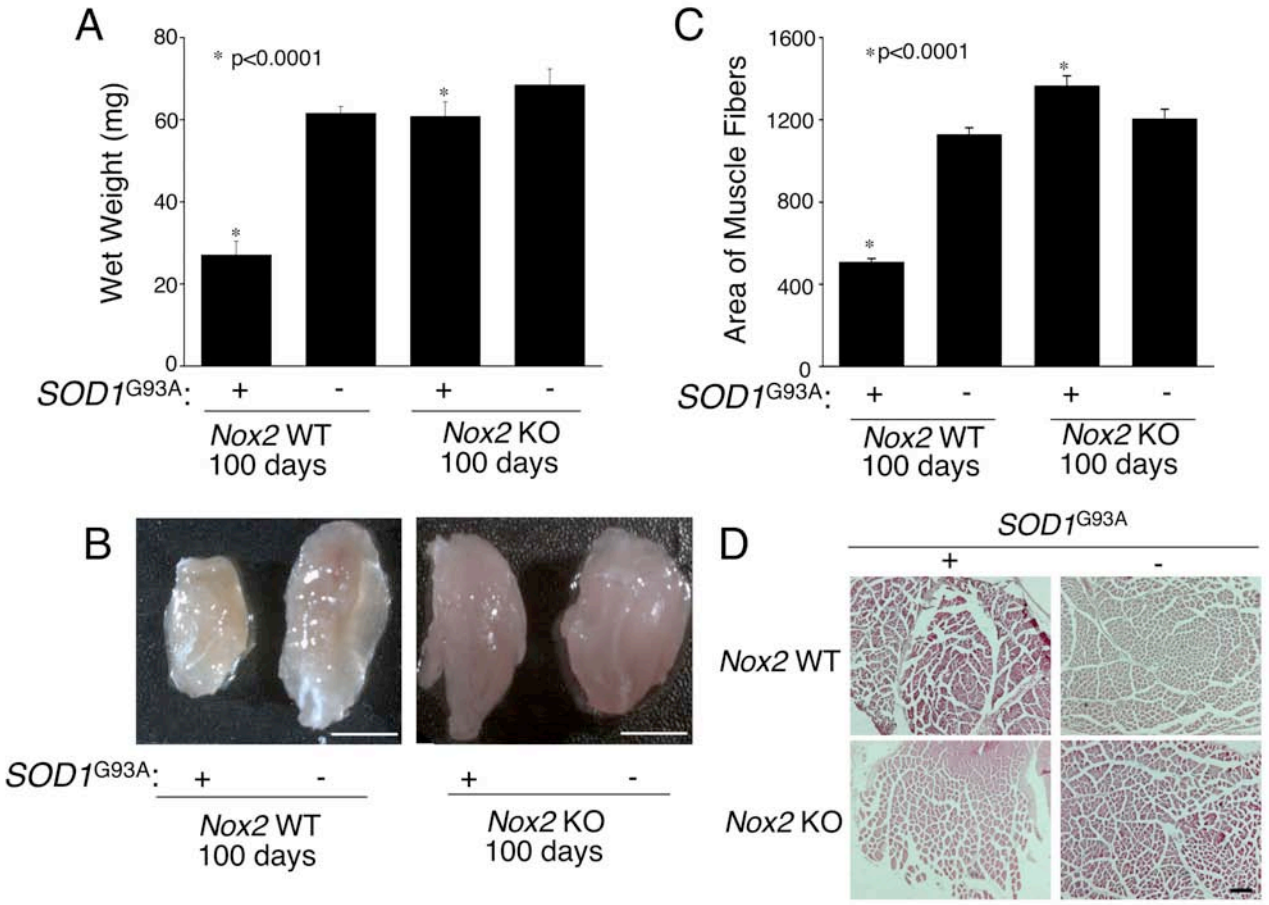

Figure S5. Hindlimb muscle atrophy is delayed in *SOD1*^{G93A}/*Nox2*-KO mice. **(A)** Wet weights of peroneous longus muscle from 100 day old mice. N=10 for each *SOD1*^{G93A} containing genotype and N=3 for each non-transgenic group. **(B)** Gross appearance of peroneous longus muscle as depicted by one representative muscle from an animal of each genotype. **(C)** Quantification of muscle fiber size determined using Image J software. **(D)** H&E stained sections of perongus longus muscle fibers.

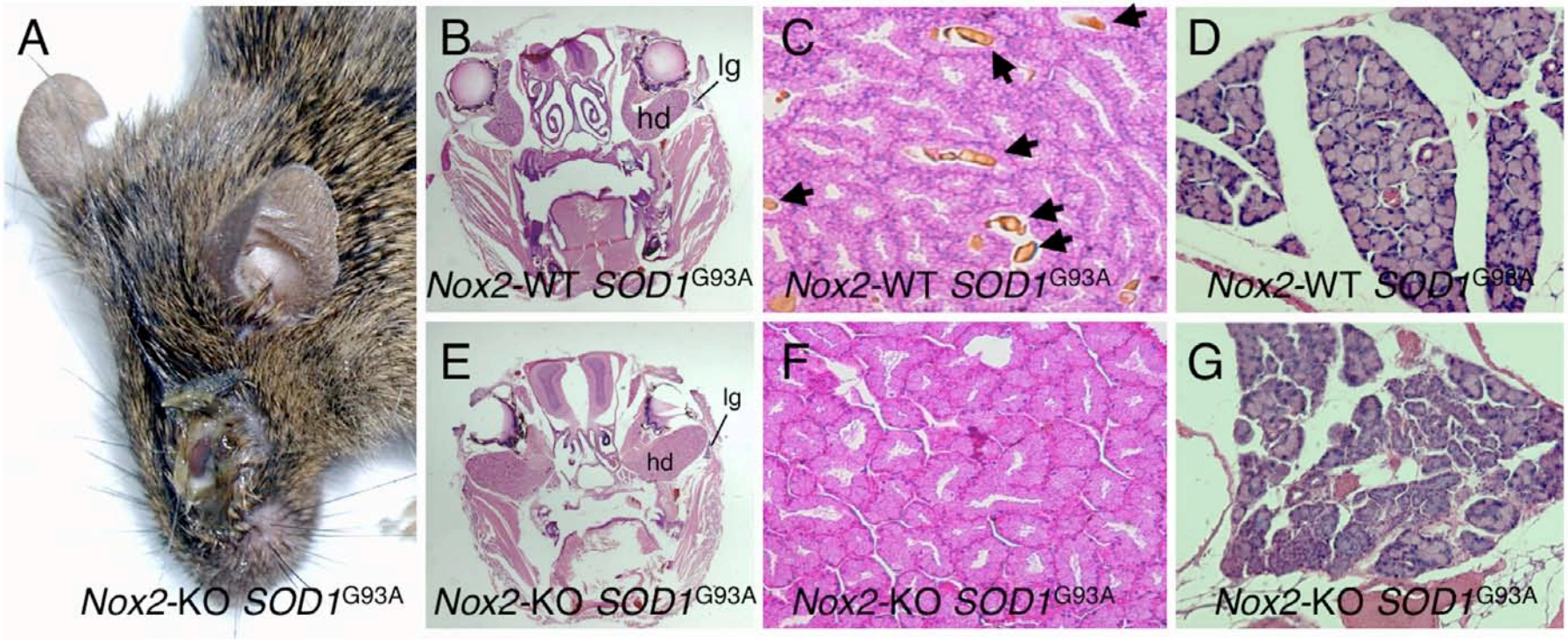

Figure S6. Histopathology of eye infection in *Nox2*-knockout *SOD1*^{G93A} transgenic mice. **(A)** Gross appearance of a *Nox2*-knockout *SOD1*^{G93A} transgenic mouse suffering from eye disease. **(B-G)** H & E stained section of the eye and related organs from **(B-D)** *SOD1*^{G93A}/*Nox2*-WT and **(E-G)** *SOD1*^{G93A}/*Nox2*-KO mice. (B and E) Low power section of the entire skull with the Harderian gland (hg) and lacrimal gland (lg) marked. (C and F) Higher power sections of the Harderian gland with intraluminal porphyrin aggregates (arrows) seen only in *SOD1*^{G93A}/*Nox2*-WT mice. (D and G) Higher power sections of the lacrimal gland demonstrating an organized acinar structure in *SOD1*^{G93A}/*Nox2*-WT mice and a more disorganized acinar structure in *SOD1*^{G93A}/*Nox2*-KO mice. The *SOD1*^{G93A}/*Nox2*-KO mouse shown in panels E-G suffered from an eye infection on gross inspection.

A

Mouse	Age of Onset (days)		
	Eye Infection	ALS Disease	Delta*
1	157	183	26
2	163	198	35
3	149	189	40
4	178	202	24
5	171	224	53
6	193	219	26
7	169	230	61
8	212	193	-19
9	240	227	-13
10	217	219	2
11	187	194	7
12	201	193	-8
13	218	228	10
14	219	223	4
Mean	**191+/-7.4**	**208+/-4.5**	**17.7+/-6.5**

*Eye Infections occurred on average 17.7 days earlier than ALS disease symptoms as indexed by 10% weight loss ($p<0.017$, paired student's t-test)

B

Figure S7. Onset of eye infection most often occurs before the onset of disease in *SOD1*^{G93A} *Nox2*-knockout mice. **(A)** The age of onset of eye infection and disease symptoms as determined by a 10% reduction in peak body weight is given for each mouse that developed an eye infection and were successfully treated with antibiotics to allow for accurate disease onset characterization. In the 5 mice that developed eye infection and died within two weeks (non-responsive to antibiotics), 2 were classified as having reached disease at the onset of the infection (as determined by a 10% reduction in peak body weight). **(B)** Photograph of the infected eye in an ALS *Nox2*-KO mouse. **(C)** Photograph showing limited hindlimb impairment in the mouse from panel B.